Getting in Tune: Resonance and Relaxation

9.1 Introduction

MRI involves three kinds of magnetic field: the main static field of the scanner (B_0), the gradients which are used for spatial localization, and the oscillating magnetic field of the RF pulses (B_1). There must be something in the body which has magnetic properties in order to interact with all these fields. So far we have deliberately avoided a detailed discussion of these properties, since we believe it's easier (and more useful practically) to understand the images first. However, the time has come to explore the protons which are essential for MRI, and on the way we will tackle some difficult concepts from quantum mechanics. We will discuss the relaxation mechanisms T_1 and T_2 in more detail. We will find that:

- hydrogen nuclei have a magnetic moment which interacts with the main field of the scanner;
- quantum mechanics controls the behaviour of the individual protons, but classical mechanics is used to describe the changes in a large collection of nuclei;
- excitation and relaxation of a collection of protons is described by the Bloch equations;
- spin–spin and spin–lattice relaxation mechanisms are due to dipole interactions, and relaxation times depend on molecular motions within the tissues;
- magnetization transfer can be observed between the bound and free water compartments in tissues;
- we can use contrast agents to modify the relaxation times of tissues, usually to create a brighter signal from pathological tissues.

9.2 Spinning Nuclei

At school, we all learned that atoms consist of electrons orbiting a central nucleus composed of neutrons and protons. As you probably know by now, MRI is derived from NMR, nuclear magnetic resonance, so we're only interested in the nucleus. In particular we want to look at the nucleus of the hydrogen atom, because of its abundance in the human body in water and other molecules. The nucleus of the hydrogen atom is a single positively charged *proton*. Something you probably didn't learn at school is that all fundamental particles (protons, neutrons, etc.) spin on their own axes, and the hydrogen nucleus is thus a continuously rotating positive charge. Basic electromagnetism tells us that a moving charge (i.e. a current) has an associated magnetic field, and so the proton generates its own tiny field known as its magnetic moment.

9.2.1 Classical Mechanics Explanation of NMR

If the proton is placed in a strong external magnetic field, it experiences a turning force, known as a torque, which tries to align the proton's magnetic moment with the main field. This is similar to a compass needle which experiences a force in the earth's magnetic field and turns so that it is aligned with the direction of the field. However, the proton is constrained by the laws of quantum mechanics. **Q**uantum **M**echanics (QM) is a branch of physics which explains some rather odd behaviours of fundamental particles, which sometimes act like individual particles and sometimes act like waves. **C**lassical **M**echanics (CM), on the other hand, works for normal-sized ('macroscopic') bodies, and for large numbers of small particles where their quantum mechanical behaviour is averaged out. Although we will have to do a bit of QM to understand why the protons don't simply align with the field, we will find that CM is quite capable of explaining almost everything else (sigh of relief!).

Since it can't align exactly with the external field, the proton continues to experience a torque which makes it *precess* around the direction of the field. This

124

precession is analogous to the wobbling of a spinning top (gyroscope) tilted slightly off axis so that it experiences a torque due to gravity. If you've never seen this, it's worthwhile buying a gyroscope from any toy store and trying to make it precess. All serious MR specialists have a gyroscope!

The precessional frequency of the protons is found to be proportional to the external magnetic field, and is given by the Larmor equation

$$\omega_0 = \gamma B_0$$

where γ is a constant called the gyromagnetic ratio, and is equal to 2.7×10^8 rad s^{-1} T^{-1}. We use ω to denote angular frequencies which are vectors, but in everyday life we use scalar frequencies denoted f; in these units the gyromagnetic ratio is 42.57 MHz T^{-1}. All the equations in this chapter use angular frequencies, but you could simply replace ω with f and use $\gamma\!\!\!\!/ = 42.57$ MHz T^{-1} to get the frequencies in megahertz. See Box '**Where's the bar?**' in Chapter 8. So the protons in a magnetic field all precess at the same Larmor frequency. This is known as a *resonance* condition. So we have the two key components for MRI, a collection of magnets (protons) and a resonance condition.

Figure 9.1 Geometric representation of the precession of the magnetic moment μ around the main field B_0.

Combining these two results we can show that the precessional frequency is given by

$$\mathbf{\omega} = -\frac{\mathrm{d}\phi}{\mathrm{d}t} = -\frac{\mathrm{d}\phi}{\mathrm{d}\mathbf{J}} \cdot \frac{\mathrm{d}\mathbf{J}}{\mathrm{d}t} = \frac{1}{J\sin\theta} \cdot -\gamma JB\sin\theta$$

$$\therefore \quad \mathbf{\omega}_0 = \gamma\mathbf{B}_0$$

The minus sign, which we quietly dropped just before the last line, is there to make sure that ω_0 defines a clockwise rotation about the z axis. So the magnetic moment precesses clockwise about B_0 at an angular frequency of ω_0 or a scalar frequency of f_0 if you prefer to use $\gamma\!\!\!\!/ = 42.57$ MHz T^{-1}.

Derivation of the Larmor Frequency: Classical Mechanics

We use vector notation in the boxes in this chapter because direction is important. Vectors are written in bold upright font, while their corresponding magnitudes are in italics, with subscripts to show component magnitudes where appropriate.

The magnetic moment $\mathbf{\mu}$ is directly proportional to the angular momentum $\mathbf{J}$

$$\mathbf{\mu} = \gamma\mathbf{J}$$

where γ is the gyromagnetic ratio. When this moment is in an external field $\mathbf{B}$ it experiences a torque and precesses about the field, its angular momentum changing according to the equation

$$\left|\frac{\mathrm{d}\mathbf{J}}{\mathrm{d}t}\right| = |\mathbf{\mu}\times\mathbf{B}| = |\gamma\mathbf{J}\times\mathbf{B}| = \gamma JB\sin\theta$$

where θ is the angle between the magnetic moment and the main field. From basic geometry (Figure 9.1) we can see that dJ is given by
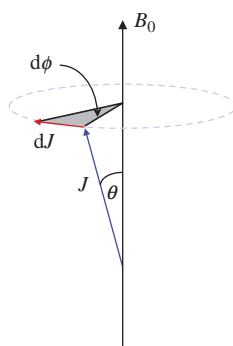
$$\mathrm{d}J = J\sin\theta\,\mathrm{d}\phi$$

9.2.2 Quantum Mechanics Explanation

So here's the QM bit. The proton's spin is said to be *quantized* in the presence of an external field, and the torque it experiences makes it precess in one of only two orientations, known in QM as 'spin states'. One state is almost aligned with the main field, and is known as *spin-up* or *parallel*. The other state is aligned almost opposite to the external field, known as *spin-down* or *anti-parallel* (see Figure 9.2). Since the magnetic moment is at an angle to the external field, the tip of its vector traces out a circle around the direction of the field (Figure 9.3), whichever orientation it is in.

How does the proton choose which orientation to precess in? It just depends on how much energy it has, since the anti-parallel direction requires slightly more energy than the parallel direction. Both states are stable, so protons are quite happy to stay in either position. However, protons can also swap between the two states simply by gaining or losing a certain amount of energy in the form of a photon (a packet of electromagnetic radiation). It turns out that the energy difference between the two states is directly

125
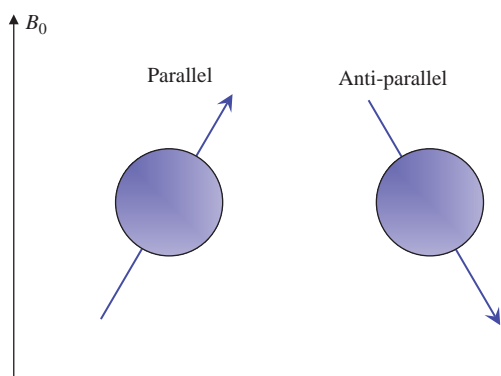
Figure 9.3 Precession of the magnetic moment.

Figure 9.2 Two possible orientations for the proton in an external magnetic field.

proportional to the strength of the external magnetic field, and from QM we can calculate exactly what the energy difference is, and thus the frequency of electromagnetic radiation required. We will find that the frequency is the Larmor frequency, just as we found from classical mechanics,

$$\omega_0 = \gamma B_0$$

So we have a link between the classical and quantum mechanical pictures, showing that the precessional frequency of the proton in a magnetic field is the same as the frequency of radiation required to cause transitions between the two states.

In the human body there are many trillions of protons; after all, we are about 75% water. So although an individual proton obeys QM, we should expect to measure their average behaviour with CM. There is a statistical distribution of protons between the two states and we find that the lower-energy state is slightly favoured, so that there are more protons spinning parallel than anti-parallel. The ratio depends on both the main magnetic field strength and (inversely) on temperature. At body temperature (37 °C) and in a 1.5 T scanner, this works out at about 1.000004, which means that for every million protons in the spin-down direction there are a million-and-four protons in the spin-up direction.

Derivation of the Larmor Frequency: Quantum Mechanics

The magnetic moment of the proton is related to the quantized angular momentum
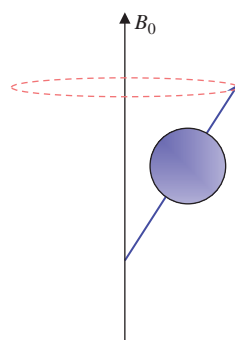
$$\mathbf{\mu} = \gamma\mathbf{J} = \gamma\hbar I$$

where I is the spin angular momentum quantum number, equal to ½ for protons, $\hbar$ is Planck's constant divided by 2π and γ is the gyromagnetic ratio. In an external magnetic field there are $2I + 1$ possible values for the angular momentum, ranging from I, $I - 1, \ldots 0, \ldots, -(I - 1), -I$. Thus for the proton there are only two possible states, with values of $\pm\frac{1}{2}$. The energy of each state (ε) is given by

$$\varepsilon = \mathbf{\mu} \cdot \mathbf{B} = \gamma\hbar I \cdot B$$

and thus we can calculate the energy difference as

$$\Delta\varepsilon = (\tfrac{1}{2} - -\tfrac{1}{2})\gamma\hbar B = \gamma\hbar B$$

De Broglie's wave equation tells us that the frequency associated with this energy is

$$\Delta\varepsilon = \hbar\omega$$

and so we can find the precessional frequency (using the subscript 0 to indicate the Larmor frequency and applied external field)

$$\hbar\omega_0 = \gamma\hbar B_0$$
$$\omega_0 = \gamma B_0$$

In equilibrium the protons are all out of phase with each other, so the tips of the magnetic moment vectors are evenly spread out around the circles (see Figure 9.4). Since there are so many protons, we can also make each vector represent the average magnetic moment of a large group of protons all precessing at exactly the same frequency, rather than an individual proton's magnetic moment. This is sometimes called an 'isochromat' of protons, but we will use the term 'spin'. This may seem like an unnecessary complication but it means that we can drop QM and just use CM from now on! The vector sum of all these spins is called the *net magnetization* M_0, which is aligned exactly with the main field B_0 (conventionally shown as the z direction). M_0 is a measurable
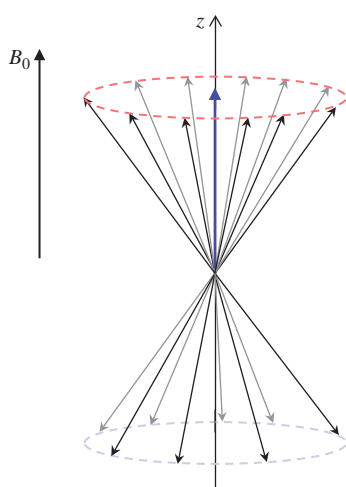
126

Figure 9.4 Average of many protons produces the net magnetization M_0.
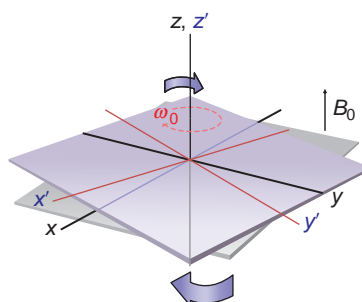

Figure 9.5 The rotating frame of reference. The coordinate system x', y', z' is considered to be rotating at the Larmor frequency in the same direction as the nuclear spins, which thus appear stationary.

magnetization which can be calculated to be of the order of microtesla (μT).

9.3 Measuring the Magnetic Moment

As we've just seen, the magnetization in the body is very small (e.g. 1 μT) compared to the main magnetic field (e.g. 1.5 T). It is virtually impossible to measure it while it is at equilibrium, lying parallel with B_0. By tipping it through 90° into the xy plane (known as the transverse plane), M_0 now generates a significant signal which can be recorded using a detector which is sensitive to magnetic fields in the transverse plane.

Population of Energy States

Whether a proton is in the parallel or anti-parallel direction depends on its internal energy. For a large collection of protons, the number in each state is given by the Boltzmann distribution:

$$\frac{N_{\text{up}}}{N_{\text{down}}} = \exp\left(\frac{\Delta\varepsilon}{k_B T}\right)$$

where k_B is the Boltzmann constant, 1.38×10^{-23} J K^{-1}. Since $\gamma\hbar B_0 \ll k_B T$ at body temperature and clinical field strengths, we can write this as

$$\frac{N_{\text{up}}}{N_{\text{down}}} = 1 + \frac{\gamma\hbar B_0}{k_B T}$$

$$\Rightarrow N_{\text{excess}} = N_{\text{up}} - N_{\text{down}} = \frac{N_{\text{total}}}{2} \cdot \frac{\gamma\hbar B_0}{k_B T}$$

This difference creates the net magnetization M_0. If we replace N_{total} with proton density ρ we will get M_0 per unit volume. We also know that the magnetic

moment of the proton has a magnitude of $\frac{1}{2}\gamma\hbar$; thus we can calculate

$$M_0 = \frac{\rho\gamma^2\hbar^2 B_0}{4k_B T}$$

Now we can calculate that water contains 6.67×10^{22} protons ml^{-1}, so we can show that at body temperature and 1.5 T we get $M_0 \approx 0.02$ μT ml^{-1}. Assuming that the human head has a volume of approximately 1500 ml and is about 80% water, $M_0 \approx 20$ μT, which is small, but measurable!

The Rotating Frame of Reference

In order to explain the effects of RF pulses and relaxation mechanisms, it is helpful to use a rotating frame of reference. However, many people automatically think about the protons in a rotating frame, and may actually find it confusing to have it explained. Physicists should read this section, but others may like to skip it for now. Refer to the Appendix if you're unsure about vector notation and the cross product.

We choose a frame rotating at the Larmor frequency about the z axis, which is defined by the direction of B_0 (Figure 9.5). In the rotating frame, spins at exactly the Larmor frequency are stationary, while those at higher or lower frequencies gain or lose phase respectively. We can describe the motion of the magnetization **M** in the new rotating frame as

$$\left(\frac{d\mathbf{M}}{dt}\right)_{rot} = \left(\frac{d\mathbf{M}}{dt}\right)_{fixed} - \boldsymbol{\omega} \times \mathbf{M}$$

where $\boldsymbol{\omega}$ is the frequency of the rotating frame. We already know that a magnetic moment precesses in an external field B (see Box 'Derivation of the Larmor Frequency: Classical Mechanics'), with its motion described by

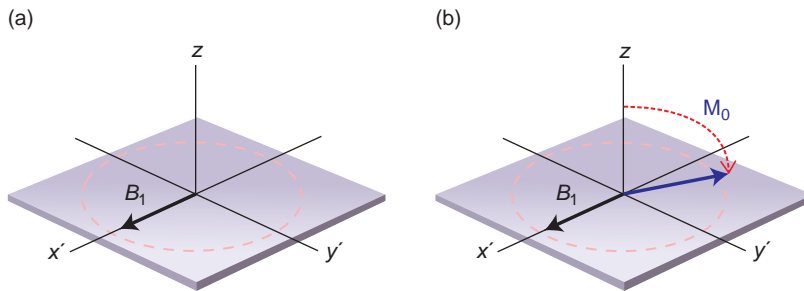$$\left(\frac{d\mathbf{M}}{dt}\right)_{fixed} = \gamma\mathbf{M} \times \mathbf{B}$$

127

(a)

(b)

Figure 9.6 (a) The RF pulse produces a fixed magnetic field B_1 in the rotating frame. (b) M_0 precesses about B_1 until the RF is switched off.

Thus we can write

$$\left(\frac{d\mathbf{M}}{dt}\right)_{rot} = \gamma\mathbf{M}\times\mathbf{B} - \boldsymbol{\omega}\times\mathbf{M}$$

$$= \gamma\mathbf{M}\times\mathbf{B} + \gamma\mathbf{M}\times\frac{\boldsymbol{\omega}}{\gamma}$$

$$= \gamma\mathbf{M}\times\left(\mathbf{B} + \frac{\boldsymbol{\omega}}{\gamma}\right)$$

The term $\boldsymbol{\omega}/\gamma$ represents a fictitious magnetic field which arises because of the rotation of the frame of reference, and thus $(\mathbf{B} + \boldsymbol{\omega}/\gamma)$ is the effective magnetic field experienced by the spins. So the motion of the magnetization in the rotating frame can be described by the same equation as in the fixed frame. This allows us to add fields due to RF pulses and predict the motion of M_0 in those conditions, if necessary using an off-resonance rotating frame. Notice that if $\mathbf{B} = B_0$ and the frame rotates at $-\omega_0$, $\mathbf{M}$ is stationary, i.e. in the basic frame rotating clockwise around z at the Larmor frequency M_0 is static. From now on we will always use x and y for the fixed laboratory frame, and x' and y' for the rotating frame. Since z and z' are aligned, we will just use z for this axis.

Figure 9.7 During the RF pulse M_0 spirals away from the z axis and down towards the transverse plane.

As you can probably guess, we tip M_0 into the transverse plane using a 90° RF pulse. What exactly is going on during the pulse though? Obviously the RF frequency used must be the Larmor frequency due to the resonance condition. The RF pulse creates a magnetic field within the transmit coil which is perpendicular to B_0 and oscillating at the Larmor frequency. In the rotating frame, this is a static field B_1 aligned along x' in the transverse plane (Figure 9.6a). M_0 moves away from the z axis until the RF pulse is switched off (Figure 9.6b). The motion of M_0 looks like a spiral since it is also precessing about the z axis (see Figure 9.7). The maths for this isn't much fun, but we can make it easier by subtracting or removing the ω_0 precession. A nice analogy for this is watching a fairground roundabout with horses going up and
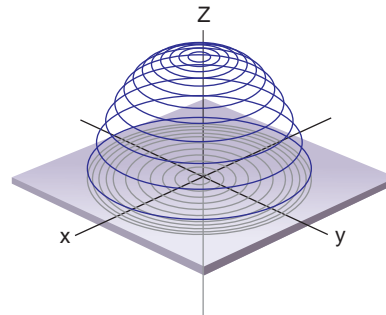
down. If you hop onto the roundabout and stand next to the horse, ignoring the outside world spinning backwards, the up-and-down motion is the only one you 'see'. Refer to Box 'The Rotating Frame of Reference' for the maths explanation.

For a simple RF pulse switched on and then off (known as a 'hard' pulse), the flip angle (α) is given by

$$\alpha = \gamma B_1 t_p$$

where B_1 is the strength of the RF magnetic field and t_p is the duration of the pulse. If M_0 ends up exactly in the transverse plane, $\alpha = 90°$ and the RF pulse is called a 90° pulse. Leaving the RF on for twice as long (or doubling its strength) would turn M_0 through exactly 180°, and the pulse would then be called a 180° pulse. Since time is always a crucial factor in MRI, we tend to just change the strength of the pulse to produce different flip angles. The RF pulse has another important effect on the spins, bringing them all into phase. This means that they all point to the same position on the precession circle.

In the Rotating Frame Again

The RF wave is produced either linearly or circularly polarized (see Chapter 10), and creates a fixed magnetic field B_1 in the rotating frame (Figure 9.6a). (A linearly polarized wave can be considered as two counter-rotating circularly polarized waves. The one

128

which is in the clockwise direction produces B_1, while the other is ignored.) The motion of M_0 in the rotating frame is given by

$$\left(\frac{d\mathbf{M}}{dt}\right)_{rot} = \gamma\mathbf{M} \times \left(\mathbf{B}_0 + \frac{\boldsymbol{\omega}}{\gamma} + \mathbf{B}_1\right) = \gamma\mathbf{M} \times \mathbf{B}_1$$

provided $\omega = -\omega_0$, i.e. the frame is rotating clockwise at ω_0. Thus the motion of M_0 will be to precess in the rotating frame about B_1 (Figure 9.6b). Note that the magnitude of B_1 is much smaller than B_0, so the precession will be much slower, typically of the order of 100 Hz (cf. 63 MHz Larmor frequency at 1.5 T). The flip angle at the end of a pulse of duration t_p will be

$$\alpha = \gamma B_1 t_p$$

To produce a 90° pulse lasting 0.25 ms, for example, we need a B_1 of only 23 µT.

Paradoxes in QM

Some useful insights into excitation can be found by considering the quantized protons, rather than just the macroscopic magnetization. Unfortunately not all the concepts can be directly translated between QM and CM, so we will point out where the usefulness of QM stops, in our opinion at least.

When the population of protons is irradiated by an RF field, protons can flip between energy levels. Spin-up protons can absorb energy to jump into the spin-down position, while those in the spin-down state are stimulated into giving up an equal amount of energy to drop into the spin-up state, and there is an equal probability of each transition. Since in equilibrium there are more spin-up protons than spin-down, the net effect will be absorption of energy from the RF wave, causing the 'temperature' of the spin system to rise. The protons' temperature is considered separately from the temperature of the surrounding tissues, known as the lattice, which will eventually come into equilibrium with the spins. We will come back to this idea when we consider spin–lattice relaxation.

Taking the simple idea of population difference and absorption of RF, it can be seen that the maximum absorption will be when all the spin-down protons have flipped into the spin-up position and vice versa. This is known as population inversion, and can be easily considered as a 180° pulse which flips the magnetization from z to –z. The definition of a 90° pulse can then be considered to be half that amount of energy, which is thought of as equalizing

the populations, leaving no magnetization along the z axis. Thus far the QM concepts seem to agree with our macroscopic observations, and they can be helpful up to this point.

However, we cannot take this picture much farther, not least because pulses larger than 180° can be used and have a measurable effect on the spin system, which is difficult to reconcile with the idea that there is a maximum absorption of energy which causes population inversion. Also, from the Boltzmann distribution, we know that increasing temperature will decrease the population difference between the two states. Thus the magnetization should decrease monotonically to zero with increasing absorption of energy. It also means that population inversion would give the spins a negative temperature, which in turn places other thermodynamic constraints on the system.

This raises some strange paradoxes which are difficult to understand in everyday terms, and we would recommend that if you want to pursue these ideas you should consult some of the physics texts listed at the end of this chapter. The good news is that many people probably have rather confused internal ideas about MRI, mixing up the concepts of classical and quantum mechanics in all sorts of odd ways, but so long as you can correctly predict the effect of changing parameters such as TR, does it matter? We think probably not!

Having rotated M_0 into the transverse plane, we measure it by detecting the voltage it induces in a receive coil which is sensitive only to magnetization perpendicular to B_0. In the laboratory frame M_0 is now precessing in the transverse plane (see Figure 9.8a), so the coil sees an oscillating magnetic field which induces a voltage varying at the Larmor frequency. The amplitude of the signal decays exponentially to zero in only a few milliseconds (Figure 9.8b), because the protons rapidly dephase with respect to each other. This signal is known as the **F**ree **I**nduction **D**ecay (FID), a rather obscure term coined by one of the original NMR researchers. In the next section we will look in more detail at what happens after excitation.

9.4 Relaxation Times

Having excited the protons in order to flip them into the transverse plane, they begin to relax back to their
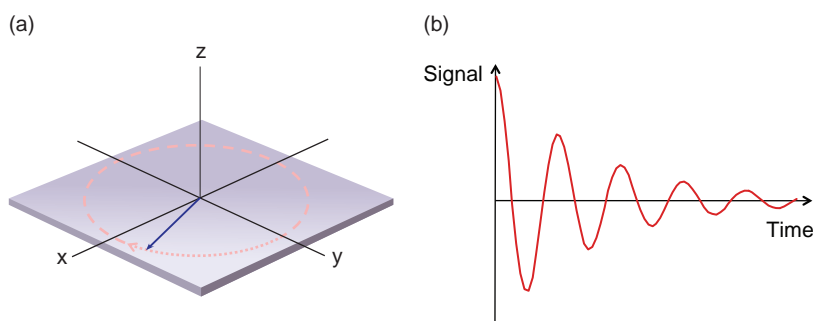
129

(a)

(b)

Figure 9.8 (a) Precession of the flipped magnetization in the transverse plane. (b) Signal induced in the receive coil – the Free Induction Decay (FID).
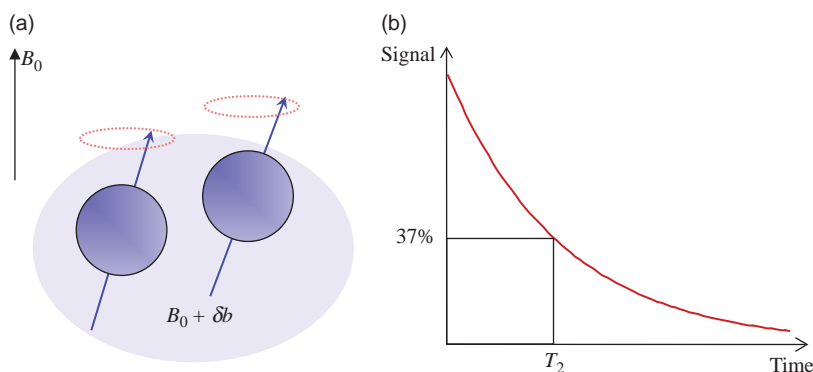
(a)

(b)

Figure 9.9 (a) As two protons come close together, they experience a change in magnetic field strength (δB) which changes their precessional frequency. (b) Because the interactions are random, the resultant transverse magnetization vector decays to zero exponentially. T_2 is the time taken for the transverse magnetization to drop to 37% of its initial size.

equilibrium position as soon as the RF pulse is switched off. There are two main features of the relaxation: a dephasing of the spins following their phase coherence after the pulse, and realignment along the z axis as they lose the energy they absorbed from the pulse.

The spins dephase because of small differences in their precessional frequencies. Thinking of the system in the rotating frame (rotating at the Larmor frequency), a slightly higher frequency will make spins dephase in the clockwise direction, while a lower frequency causes an anticlockwise phase angle. Anything that changes a spin's frequency from the Larmor frequency will add to the dephasing. For the FID, the dominant effect is the unavoidable inhomogeneity in the main magnetic field. A second effect is formed by the interactions between spins as they move around within the tissues. It is this interaction that we call *spin–spin relaxation*, characterized by the spin–spin relaxation time T_2, which is independent of the magnet in which it is being measured and (for practical purposes) largely independent of field strength.

To understand T_2, imagine a system of excited protons in a perfect magnetic field, free to move around in a random fashion. They all precess in the transverse plane, ignoring the relaxation back to the z axis for now. So long as they are evenly distributed around the volume, they are all precessing at the Larmor frequency and remain in phase in the rotating frame. However, if two protons come close together, each of them experiences a slightly higher or lower magnetic field, as the magnetic moment of the other proton adds or subtracts from the main field (Figure 9.9a). Their precessional frequencies change instantaneously to match the 'new' field, and each proton will dephase with respect to the Larmor frequency. When they move apart again they both return to the Larmor frequency, but the phase angles they acquire during the interaction are irreversible. Over time each proton will interact with many thousands of other protons, and the phase angles become larger and larger until all the protons are out of phase with each other. The vector sum of the magnetic moments, which is the signal we detect in the MR receiver, gradually decays from a maximum

130

Table 9.1 Selection of T_1 and T_2 values for tissues at 0.5 T, 1.5 T and 3 T. All values measured in vivo from human tissues

	T_1 (ms)			T_2 (ms)		
Tissue	0.5 T	1.5 T	3 T	0.5 T	1.5 T	3 T
White matter	520[f]	560[a]	832[i]	107[b]	82[c]	110[i]
Grey matter	780[f]	1100[a]	1331[i]	110[b]	92[c]	80[i]
CSF	–	2060[e]	3700	–	–	–
Muscle	560[g]	1075[d]	898[h]	34[g]	33[g]	29[h]
Fat	192[b]	200[b]	382[h]	108[b]	–	68[h]
Liver	395[b]	570[e]	809[h]	96[b]	–	34[h]
Spleen	760[b]	1025[e]	1328[h]	140[b]	–	61[h]

Notes:
[a] Steinhoff S, Zaitsev M, Zills K, Shah NJ (2001). 'Fast T_1 mapping with volume coverage'. *Mag Reson Med* 46: 131–140.
[b] Bottomley PA, Foster TH, Argersinger RE, Pfeifer LM (1984). 'A review of normal tissue hydrogen NMR relaxation times and relaxation mechanisms from 1–100 MHz: dependence on tissue type, NMR frequency, temperature, species, excision and age'. *Med Phys* 11: 425–448.
[c] Pfefferbaum A, Sullivan EV, Hedehus M, Lim KO (1999). 'Brain gray and white matter transverse relaxation time in schizophrenia'. *Psychiat Res* 91: 93–100.
[d] Venkatesan R, Lin W, Haacke EM (1998). 'Accurate determination of spin-density and T_1 in the presence of RF field inhomogeneities and flip-angle miscalibration'. *Mag Reson Med* 40: 592–602
[e] Bluml S, Schad LR, Stepanow B, Lorenz WJ (1993). 'Spin–lattice relaxation time measurement by means of a TurboFLASH technique'. *Mag Reson Med* 30: 289–295.
[f] Imran J, Langevin F, Saint Jalmes, H (1999). 'Two-point method for T_1 estimation with optimized gradient-echo sequence'. *Magn Reson Imag* 17: 1347–1356.
[g] de Certaines JD, Henrikson O, Spisni A, Cortsen M, Ring PB (1993). 'In vivo measurements of proton relaxation times in human brain, liver, and skeletal muscle: a multi-centre MRI study'. *Magn Reson Imag* 11: 841–850.
[h] de Bazelaire CM, Duhamel GD, Rofsky NM, Alsop DC (2004). 'MR imaging relaxation times of abdominal and pelvic tissues measured in vivo at 3.0 T: preliminary results'. *Radiology* 230: 652–659.
[i] Wansapura JP, Holland SK, Dunn RS, Ball WS Jr (1999). 'NMR relaxation times in the human brain at 3.0 tesla'. *J Magn Reson Imaging* 9: 531–538.

immediately after the excitation pulse down to zero (Figure 9.9b). Since their motion is random, the dephasing is an exponential decay process, which we call spin–spin relaxation.

Although the transverse magnetization decays, there is no net loss of energy in spin–spin relaxation. To lose energy, the protons must interact with the surrounding tissues (Figure 9.10), known as the lattice, which can absorb the energy and disperse it via blood flow. As the protons lose the extra energy from the RF pulse, they gradually return to the equilibrium populations in the spin-up and spin-down states, so that eventually the magnetization along the z axis, M_z, is back to M_0. This is known as *spin–lattice relaxation*, characterized by the spin–lattice relaxation time T_1. Unlike T_2, T_1 changes with field strength, getting longer as the field strength increases, and T_1 is always longer than T_2. Table 9.1 shows some approximate values at 0.5 T, 1.5 T and 3

T (use these with caution – remember that in vivo measurements are often inaccurate).

Since we consider the net magnetization being flipped through 90° by the RF pulse, it is tempting to think of the relaxation processes as simply being the reverse, with M_0 slowly turning through –90° back to its equilibrium position. This would explain the gradual loss of transverse magnetization and recovery of the longitudinal magnetization. However, it would also imply that T_1 and T_2 must be equal to each other, and we know that this is not the case in biological tissues. Many textbooks do not make this clear enough, showing T_1 and T_2 curves without time scales so it is difficult to see that two separate processes are at work. T_2 dephasing happens quickly, so the transverse magnetization is zero after only a few hundred milliseconds. T_1 relaxation is much slower and it may take several seconds before M_0 is fully restored along the z axis.
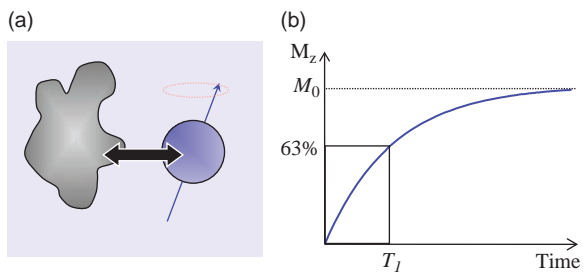
Figure 9.10 (a) The spins can transfer energy to the surrounding lattice, allowing them to relax back to equilibrium. (b) The process is random, so the recovery of M_z to M_0 is controlled by an exponential. T_1 is the time taken for the magnetization to recover to 63% of its equilibrium value.
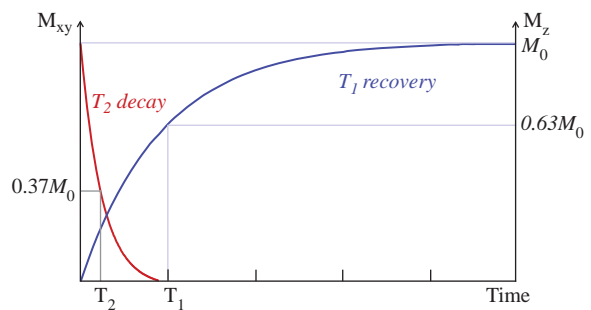

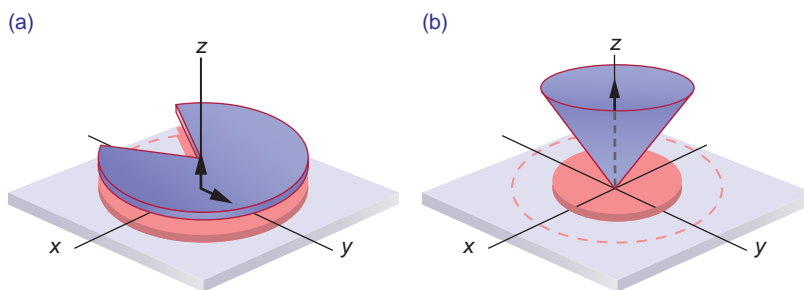Figure 9.11 T_1 and T_2 relaxation occur simultaneously, but T_2 is much quicker than T_1.

Figure 9.12 T_2 relaxation causes rapid fanning out of the protons in the transverse plane (a). T_1 is much slower, and can be thought of as an umbrella closing up (b).

If we plot both curves on the same graph for a tissue with $T_1 \approx 5 \times T_2$ (Figure 9.11) you can see the differences in the time scales for these two processes. Looking at Table 9.1 you can see that in most tissues T_1 is several times longer than T_2. It is better to use a more specific mental picture in which the protons rapidly dephase like a fan opening up in the transverse plane, before folding up slowly towards the z axis like an umbrella closing (see Figure 9.12). Compare this with the simplistic idea of M_0 rotating back and forth between the z- and y-axes, and you will realize that too much simplification can be seriously misleading. Although the full picture takes a bit more effort to think about, it won't let you down!

9.5 Creating Echoes

In MRI we never measure the FID directly; instead we use two types of echo, gradient (GE) and spin echoes (SE). In each case the sequence starts with an RF excitation pulse, 90° in the case of SE and

smaller angles in GE. We will explain gradient echoes first.

In the GE sequence (Figure 9.13), we apply a negative gradient lobe immediately after the excitation pulse. This causes rapid dephasing of the transverse magnetization, much faster than the normal FID. After the negative lobe we apply a positive gradient, which simply reverses the magnetic field gradient. Spins that were precessing at a low frequency due to their position in the gradient will now precess at a higher frequency because the gradient will now add to the main field, and vice versa. Spins which were previously dephasing now begin to rephase, and after a certain time they will all come back into phase along the y' axis forming the gradient echo. However, the positive gradient only compensates for the dephasing caused by the negative gradient lobe, it does not refocus dephasing due to the main magnetic field inhomogeneities or spin–spin relaxation (which is explained in the next section). The height of the echo (S_{GE}) is thus determined by the FID decay curve which depends on T_2^*
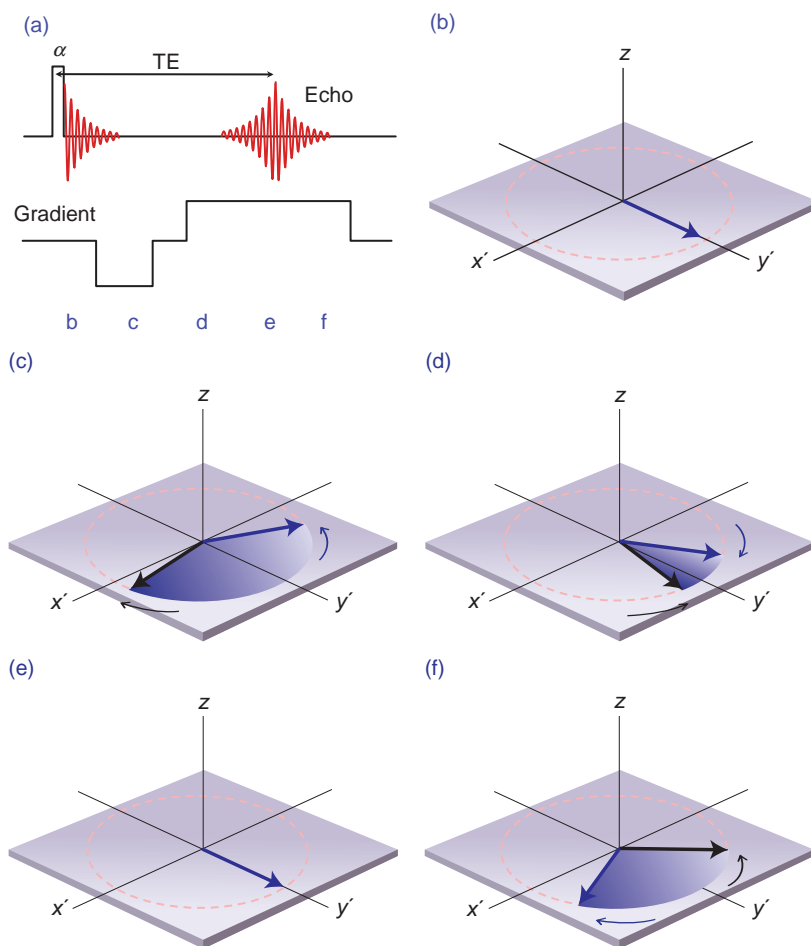
132

$$S_{GE} = S_0 \exp\left(-\frac{TE}{T_2^*}\right)$$

where S_0 is the initial height of the FID. T_2^* is a composite relaxation time which includes T_2, inhomogeneities due to the main field and tissue susceptibility, and diffusion of the protons.

In the spin-echo sequence (Figure 9.14) we leave the spins to dephase naturally after the 90° pulse for a certain time. Then we apply a 180° pulse on the $+y'$ axis which flips all the spins through 180° about the y' axis. It does not change the precessional frequencies of the spins, but it does reverse their phase angles. Spins which were in a lower magnetic field strength will have been dephasing anticlockwise; the 180° pulse flips them over and they now appear to have been in a higher magnetic field and have dephased clockwise. Similarly, spins which were

dephasing clockwise will appear to have been in a lower magnetic field and dephased anticlockwise. Assuming that the spins do not move too far within the imaging volume, they will continue to experience the same magnetic field inhomogeneities and continue to dephase in the same direction. After a time equal to the delay between the 90° and the 180° pulse, all the spins will come back into phase along the $+y'$ axis, forming the spin echo. The phase-reversal trick means that the echo height will only depend on T_2 and diffusion, and not on the magnetic field inhomogeneities or tissue susceptibilities. Provided we keep the echo times fairly short, the diffusion component is negligible and we find that the signal S_{SE} is dependent on T_2:

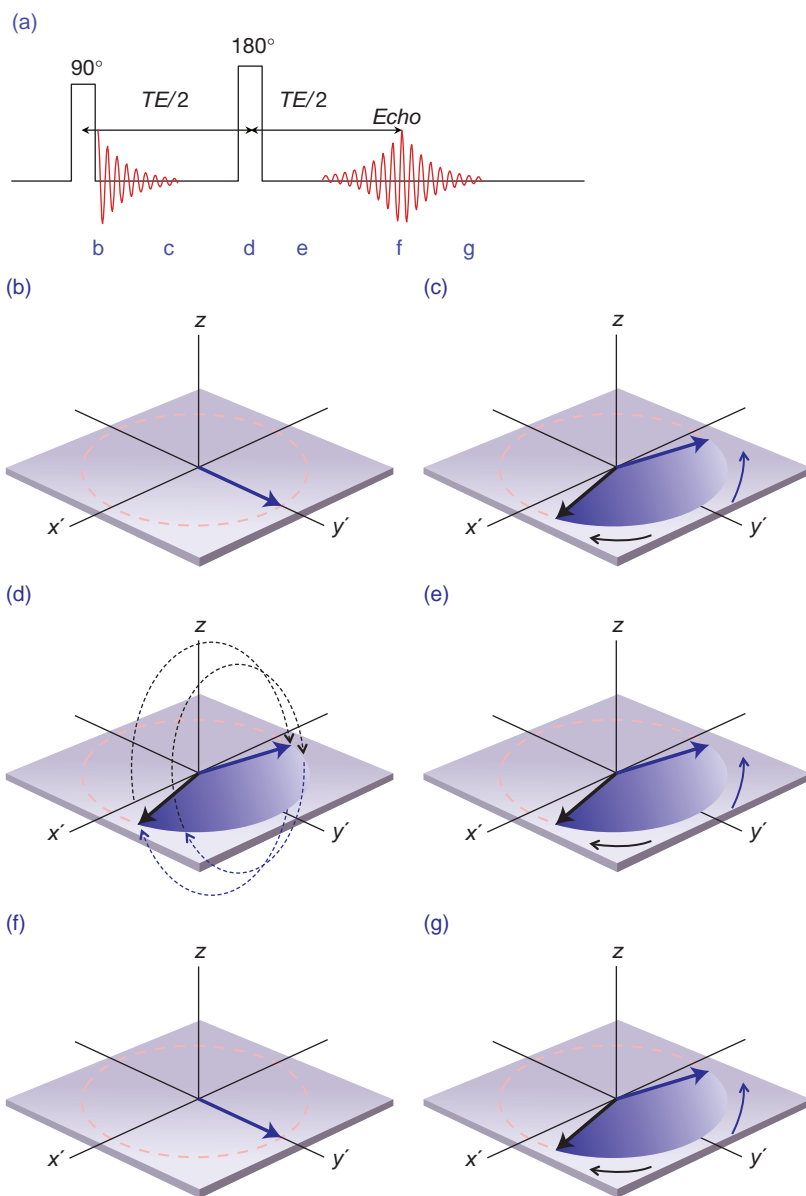$$S_{SE} = S_0 \exp\left(-\frac{TE}{T_2}\right).$$

(a)

Figure 9.14 (a) Spin-echo pulse sequence. Spins initially in phase (b) dephase naturally (c) until the 180° pulse is applied (d). Immediately after the pulse their phases are reversed, but they continue to dephase in the same direction (e) forming an echo (f) and then dephasing again (g).

RF Phase Angles: Which Axis?

You may find that other texts show the 180° pulse on the +x′ axis so that the fan of dephasing protons is flipped a further 180° and creates a spin echo along the −y′-axis, i.e. a negative echo (but then of course we take the magnitude for the final image intensity). Why have we done it differently? Well partly because we have found, over many years of giving lectures, that people find the negative echo an extra complication, and we can avoid that just by putting the 180° pulse on +y′. Both forms create a spin echo of the same height, the only difference is in the direction of the vectors. It is also because multi-echo sequences always put the 180° pulses on +y′ instead of +x′, which partially compensates for imperfections in the RF pulse.

134

9.5.1 The 'Runners on a Track' Analogy (Slightly Reworked)

You may have come across this analogy to describe the spin echo in other textbooks or lectures. It is explained by saying that the runners all start at the same time (analogous to the 90° pulse exciting all the protons), but because they run at different speeds, after a while they are spread out along the track. The 180° pulse is like turning all the runners around at this point, so that they all have to run back to the starting point. Assuming they all continue to run at the same speeds, after an equal time they will all cross the starting point together – analogous to the protons coming back into phase to create the echo.

We can modify this slightly to explain the differences between spin echo and gradient echo, and also show why the echo heights depend on T_2 and T_2^* respectively. First, suppose that as well as running at different speeds, the runners get tired at different rates, so they tend to slow down. Also imagine that the track is not flat but rather lumpy, and that it is different in each lane. To explain the spin echo first, let the runners start together running in one direction; after a while they are spread out due to the differences in their running speeds and the track conditions in each lane. When the 180° pulse is applied the runners all turn around and run back towards the starting point, and magically the track conditions are reversed: the bad lanes become perfect, the good ones become difficult. So if the runners all go at the same speeds as before, the effects of the track will be evened out and they will all cross the starting point together. Since they get tired though, they don't manage to maintain their speeds, and in fact we only get some of them back at the same time.

To extend the analogy to gradient echo, the gradient reversal is the turning point instead of the 180° pulse. This time, however, the track conditions don't get fixed and the runners who had bad lanes to start with have to run back under the same conditions. As well as tiredness slowing them down, the lane conditions alter their performance. At the echo time, even fewer of the runners are back at the starting point. In this extended analogy, the runners' different tiredness rates are analogous to T_2 and the lane conditions are analogous to the magnetic field inhomogeneities.

9.6 Relaxation Time Mechanisms

The time difference between T_1 and T_2 is extremely important in all MR imaging or spectroscopy. We always use a repeated sequence of RF and gradient pulses, with a repetition time (TR). Consider the simple case of a repeated 90°–TR–90°–TR sequence; if TR is at least five times the longest T_1 of the tissues, all tissues will be back to equilibrium before the next 90° and the signal in the transverse plane will depend only on the proton density. However, if TR is shorter, M_z will not have had sufficient time to grow back to M_0 and a smaller signal will be flipped into the xy plane. (Provided TR is still longer than five times T_2, there will be no transverse magnetization to confuse the issue. When TR is so short that there is still M_{xy} before the next pulse, there is a more complex situation which will be discussed in Chapter 13.) This loss of signal is known as *saturation*.

To help fix this new picture of relaxation in your mind, let us review the way TR affects T_1 contrast in spin-echo images (first discussed in Section 3.5), illustrated in Figure 9.15. Assuming we start from full relaxation, the initial 90° pulse rotates all the longitudinal magnetization into the transverse plane. After the spin echo has been formed, T_2 decay continues while M_z grows in the z direction – the red vector has a longer T_1 than the blue one, so it recovers more slowly. When the second 90° pulse is applied, provided $TR > 5 \times T_2$, M_{xy} is zero, but T_1 recovery is not complete. Only the z magnetization will be flipped into the transverse plane to create signal for the next echo. Both M_z go back to zero and begin to relax back to equilibrium again. After a further TR, both vectors have recovered to exactly the same amount, so the third and all subsequent excitations create a steady signal height which is T_1-weighted.

Strictly speaking, a dummy excitation is needed for a spin-echo sequence to reach the *steady state*. However, the normal linear phase encoding scheme means that the first echo does not affect contrast in the final image, so it is rarely done in practice. Gradient-echo sequences are another matter: the number of pulses needed to reach a steady state depends on TR and the flip angle, as well as the relaxation times of the tissues (see Section 13.1 and Figure 13.1).

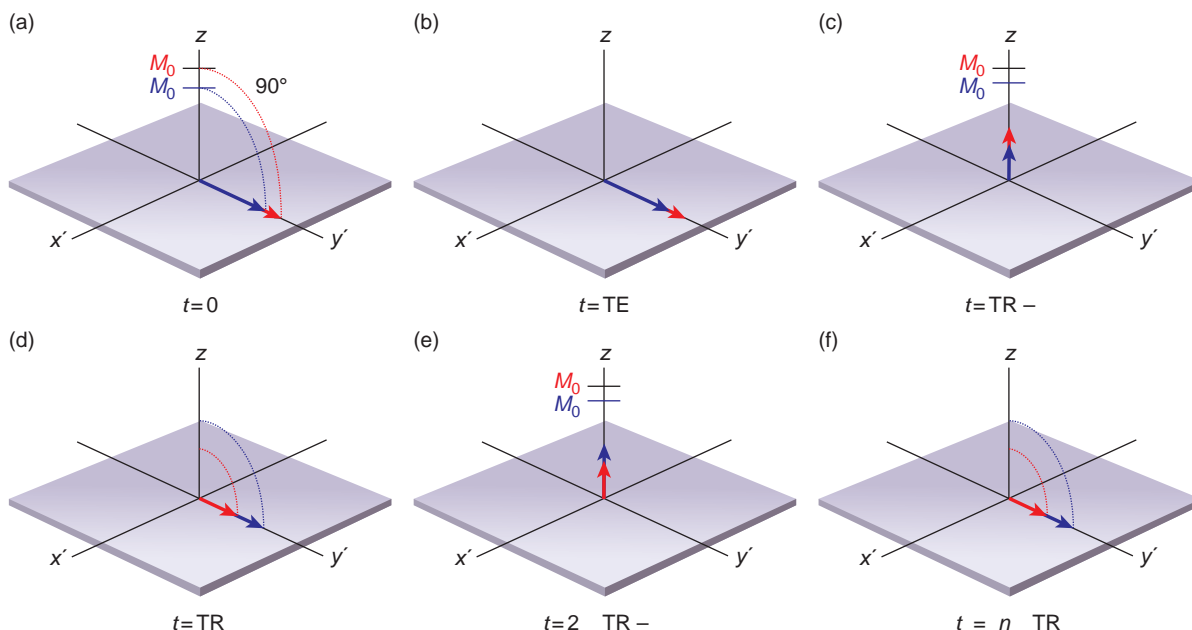In this section we will consider the interactions between protons and their environment which cause

135

Figure 9.15 (**a**) During the first 90º pulse, both M_0 are rotated into the transverse plane, producing M_{xy} (**b**). (**c**) After $5 \times T_2$, M_{xy} has decayed to zero while M_z recovers from zero with T_1 relaxation. When the second 90º pulse is applied after time TR, (**d**) reduced signals are rotated into the transverse plane. (**e**) After another TR, both M_z have recovered to the same height as before, so the third 90º pulse creates the same T_1-weighted signal in the transverse plane (**f**).

spin–spin and spin–lattice relaxation. Much of our understanding of relaxation is based on work published in 1948 by **B**loembergen, **P**urcell and **P**ound, which is usually known as the BPP theory of relaxation. To understand this you must be familiar with the concept of molecular motions: every atom or molecule is rotating, vibrating and translating (i.e. moving from one position to another) in random directions. Not only that, molecules change their motion rapidly, so they will be vibrating one second and rotating the next, because they collide with each other. Actually a molecule spends only a tiny fraction of a second in a particular state of motion, as little as 10^{-12} s, before suffering a collision which changes its motion to something different. This is known as the correlation time τ_c of the molecule, and if you use the standard idea of gases, liquids and solids you will be able to imagine that solids tend to have very long correlation times (molecules are closely packed together and move slowly), while gases at the other extreme have shorter τ_c (molecules are further apart and move quicker). τ_c is also affected by temperature, with higher temperatures giving shorter correlation times.

136

The Bloch Equations

Bloch derived a set of differential equations which describe the changes in the magnetization during excitation and relaxation. They are sometimes called 'phenomenological' because they describe the phenomenon that we detect in the receive coil, rather than being derived from fundamental principles. Note that they are based entirely on classical mechanics. We start with

$$\frac{d\mathbf{M}}{dt} = \gamma \mathbf{M} \times \mathbf{B} = \gamma \begin{bmatrix} (M_y B_z - M_z B_y)\mathbf{i} \\ +(M_z B_x - M_x B_z)\mathbf{j} \\ +(M_x B_y - M_y B_x)\mathbf{k} \end{bmatrix}$$

We use a general expression for B which includes a static field along z and a second field rotating in the transverse plane

$$B_x = B_1 \cos \omega t$$
$$B_y = -B_1 \sin \omega t$$
$$B_z = B_0$$

and add terms which account for the observed relaxations T_1 and T_2, giving

$$\frac{dM_x}{dt} = \gamma(M_y B_0 + M_z B_1 \sin \omega t) - \frac{M_x}{T_2}$$

$$\frac{dM_y}{dt} = \gamma(M_x B_1 \cos \omega t - M_x B_0) - \frac{M_y}{T_2}$$

$$\frac{dM_z}{dt} = -\gamma(M_x B_1 \sin \omega t + M_y B_1 \cos \omega t) - \frac{M_z - M_0}{T_1}$$

These can then be solved with appropriate limiting conditions; for example, immediately after the RF pulse is switched off, $B_1 = 0$ and the solutions are

$$M_x(t) = [M_x(0) \cos \omega_0 t + M_y(0) \sin \omega_0 t] \cdot \exp\left(\frac{-t}{T_2}\right)$$

$$M_y(t) = [M_y(0) \cos \omega_0 t - M_x(0) \sin \omega_0 t] \cdot \exp\left(\frac{-t}{T_2}\right)$$

$$M_z(t) = M_z(0)\exp\left(\frac{-t}{T_1}\right) + M_0\left[1 - \exp\left(\frac{-t}{T_1}\right)\right]$$

If the system was initially in equilibrium and the RF pulse was a 90° pulse applied along the +x' axis, $M_x(0) = M_z(0) = 0$ and $M_y(0) = M_0$, giving the results

$$M_x(t) = M_0 \sin \omega_0 t \cdot \exp\left(\frac{-t}{T_2}\right)$$

$$M_y(t) = M_0 \cos \omega_0 t \cdot \exp\left(\frac{-t}{T_2}\right)$$

$$M_z(t) = M_0\left[1 - \exp\left(\frac{-t}{T_1}\right)\right]$$

In complex notation this is

$$M_{xy}(t) = M_0\exp(i\omega_0 t) \cdot \exp\left(\frac{-t}{T_2}\right)$$

$$M_z(t) = M_0\left[1 - \exp\left(\frac{-t}{T_1}\right)\right]$$

This tells us that the x and y magnetizations oscillate at the Larmor frequency while decaying with time constant T_2, while the z magnetization simply grows from zero back to M_0.

The Spectral Density Function and Water Binding

Statistical methods can be used to show that a collection of molecules with an average correlation time τ_c will have a range of motional frequencies described by something called the spectral density function $J(\omega)$. This simply shows the number of nuclei that tumble at each frequency. Figure 9.16 shows $J(\omega)$ for three materials with long, medium and short
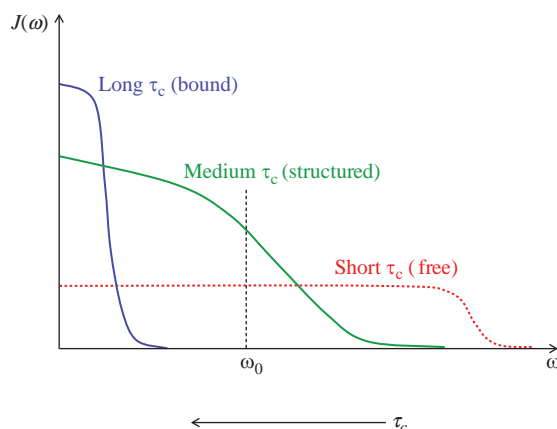

Figure 9.16 Spectral density functions $J(\omega)$ for three substances with varying correlation times τ_c.

τ_c. Long τ_cs mean that molecules spend a relatively long time in a particular motional state before suffering a collision, and we can see that most of the motional frequencies are very low. With shorter τ_cs, molecules are highly mobile and are changing their motional states with high frequencies. Notice that the Larmor frequency of most clinical MR systems, tens of MHz, is in the middle of the frequency range. We will come back to spectral density functions in the next two sections.

In biological systems, water is rarely a free liquid except in CSF, blood or cysts. Large molecules such as polysaccharides and proteins form hydration layers, layers of water molecules which are closely bound to the surface of the larger molecule. There is a continuous variation of 'binding', from the tightly bound protons close to the surface to the 'free' protons furthest away from large molecules. In addition, protons do not stay in one place but can be exchanged between different molecules. As they swap places, their bound properties change, and this changes the signal that they produce. This is known as free exchange of protons, and it means that the measured signal is a mixture of all the different signals, ranging from fully bound to completely free.

9.6.1 Spin–Lattice Relaxation

We know that an RF pulse on average promotes protons from the low-energy state to the high-energy state, causing a net absorption of energy. T_1 relaxation is the loss of the extra energy from the spin

137

system to the surrounding environment, or 'lattice' (hence 'spin–lattice' relaxation time). However, the high-energy state is a stable position for the proton and it does not return to the lower state spontaneously but requires an external stimulating field. Since the external B_1 field has been switched off, where does this field come from? As we have hinted in the previous section, it comes from neighbouring protons or other nuclei or molecules, which have magnetic moments. In water the nearest adjacent nucleus will be the other hydrogen atom on the same molecule. Therefore, relaxation will primarily arise through the magnetic moment that one hydrogen nucleus 'sees' as it tumbles relative to the moment of the other hydrogen nucleus. This is often called an intra-molecular dipole–dipole interaction (a dipole is simply a magnetic field with two poles, north and south – another term for a magnetic moment).

We have already seen that molecules have a range of motional frequencies, described by the spectral density function (see Box 'The Spectral Density Function and Water Binding'). So the magnetic moments of these molecules will also have a frequency distribution. In order to induce the transitions needed for T_1 relaxation, the fluctuations have to be at the Larmor frequency, in the same way that the external B_1 field has to oscillate at the Larmor frequency. So we can predict that the more protons that tumble near the Larmor frequency the more efficient the T_1 relaxation will be. For example, more protons with intermediate binding tumble at the Larmor frequency than protons in either free fluids or bound in hydration layers. Hence the T_1s of such protons are short while both bound and free protons have long T_1s. The spectral density function also predicts that T_1 is frequency dependent, since a decrease in the strength of the static magnetic field will decrease the Larmor frequency. There will be more protons tumbling at the new lower Larmor frequency so the T_1 will be shorter.

9.6.2 Spin–Spin Relaxation

We know that T_2 relaxation arises from the exchange of energy between spins, hence the term 'spin–spin relaxation'. No energy is actually lost from the spin system but the decay of transverse magnetization arises from the loss of phase coherence between spins, which arises from magnetic field inhomogeneities. These inhomogeneities may be either intrinsic or extrinsic, i.e. internal to the proton system or external in the scanner. Only the intrinsic inhomogeneities contribute to T_2.

Our description of molecular motions can also be used to describe the mechanism of T_2 relaxation. When molecules are tumbling very rapidly (i.e. free protons with short τ_c) then a particular dipole will see the local magnetic field as fluctuating very rapidly and effectively averaging out over a few milliseconds. This results in a relatively homogeneous local field and little dephasing, and is sometimes termed 'motional averaging'. Conversely, a slowly tumbling molecule (bound protons close to large molecules) will see a relatively static magnetic field inhomogeneity and will be more effectively dephased with respect to other protons.

In terms of the spectral density function, we see that T_2 is affected by low-frequency motions as well as those at the Larmor frequency (for comparison, T_1 is only affected by Larmor frequency fluctuations). Bound protons have very short T_2 values, so short that even at the shortest echo times we can use in MRI their signals are completely decayed to zero. Free protons in bulk fluids have the longest T_2s while those with intermediate binding have medium T_2 relaxation times.

A Magic Moment with Magic Angles

In highly ordered collagen-rich tissues such as tendon and ligament, water molecules bound to the collagen relax rapidly due to dipole–dipole interactions. Normally this results in a very short T_2 of less than 1 ms and the usual MR appearance of these structures is dark. However, the strength of the relaxation mechanism depends upon the angle of the collagen fibres with the B_0 field. At an angle approximately 55° or 125° to B_0 the interactions are very much reduced, resulting in an increase in T_2 and a hyperintense signal intensity on T_1w or PDw images. At the so-called magic angle, the T_2 of these tissues can be of the order of 20 ms. When the hyperintensity is unwanted this is known as the *magic angle artefact*, which is well recognized by musculoskeletal radiologists. Alternatively, scanning at the magic angle offers the opportunity to investigate tendon and ligament function and pathology, although in a conventional closed bore scanner it is extremely hard to arrange for the appropriate geometry. Studies on tendon and ligament properties have been carried out ex vivo (Figure 9.17).
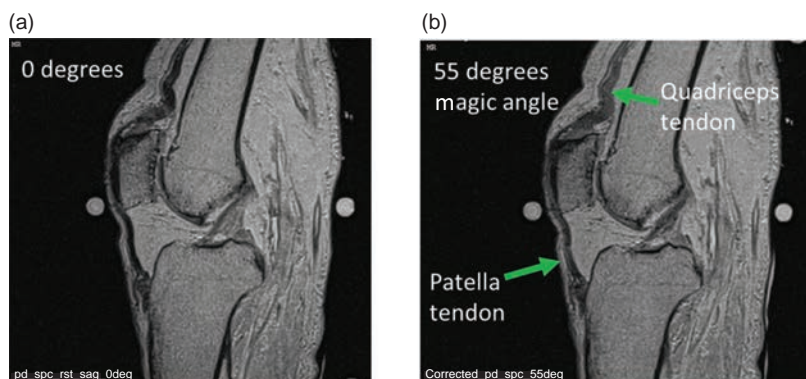
138

(a)

(b)

Figure 9.17 Cadaveric knee at 0° and the magic angle (55°) showing intensity increases (arrowed) in collagen-rich structures such as the quadriceps tendon and patellar tendon. Courtesy of K. Chappell, Imperial College, London.

9.6.3 BPP Theory for Body Tissues

We can summarize the BPP relaxation theory in terms of three tissue types. Let us start with water molecules that are essentially 'free' in solution, e.g. CSF, in which there is a reasonably uniform number of protons tumbling over a wide range of frequencies. There is only a small number tumbling at the Larmor frequency so T_1 relaxation is relatively inefficient, i.e. T_1 relaxation times are long. Similarly there is only a small number tumbling at very low frequencies; therefore, T_2 relaxation is also inefficient, i.e. T_2 relaxation times are long.

If we now consider water molecules that are 'bound' to larger macromolecules through the formation of a hydration layer, e.g. myelin, then there are a large number of protons tumbling at very low frequencies because their motion is restricted by the binding. In this case T_2 relaxation is very efficient (very short T_2s) and T_1 relaxation very inefficient (long T_1s). In fact, the T_2 relaxation times are so short that these molecules are 'invisible' with conventional MR imaging equipment, because by the time we collect echoes at even the shortest echo times their signals have fully decayed.

The third case to consider is when a proton is in the intermediate situation between bound and free; this is sometimes termed 'structured'. Now there are a large number of protons tumbling at the Larmor frequency and T_1 relaxation will be the most efficient. T_2 relaxation will be intermediate between bound (short T_2) and free (long T_2). Most body tissues are in the structured water category. Lipids are a special case: due to the much larger size of unbound lipid molecules, their protons intrinsically tumble at lower frequencies, i.e. more tumble at the Larmor frequency and they therefore have short T_1 relaxation times.

Exchanging Protons

In describing relaxation mechanisms in this way we have ignored the fact that in reality water molecules are in fast exchange between the three states, i.e. over the time scale of an MRI scan a water proton will wander between bound, structured and free tissues. The proportion of time spent in each state will, in effect, be the same as the proportion of water in each state. The observed relaxation time is therefore a weighted-mean of the relaxation time of each fraction

$$\frac{1}{T_1{}^{obs}} = \frac{F^{bound}}{T_1{}^{bound}} + \frac{F^{struct}}{T_1{}^{struct}} + \frac{F^{free}}{T_1{}^{free}}$$

$T_1{}^{bound}$ is very long, so only a small fraction of tissue water needs to be in the bound compartment to reduce the observed T_1. A similar equation can be written for observed T_2s. While the bound compartment cannot be directly observed, it may however be investigated using magnetization transfer techniques (see Section 9.6.4). Water binding is not the only mechanism to affect relaxation in tissues. The presence of paramagnetic material, either intrinsic (blood breakdown products) or extrinsic (exogenous contrast agents such as gadolinium), can have a profound effect on observed relaxation times, as we will see in Section 9.6.4.

9.6.4 Magnetization Transfer and *J*-Coupling

Magnetization **T**ransfer (MT) provides an additional source of contrast for certain tissues. A physical explanation is given in Box 'Getting Bound Up: MT Explained'. MT can be exploited in imaging to reduce
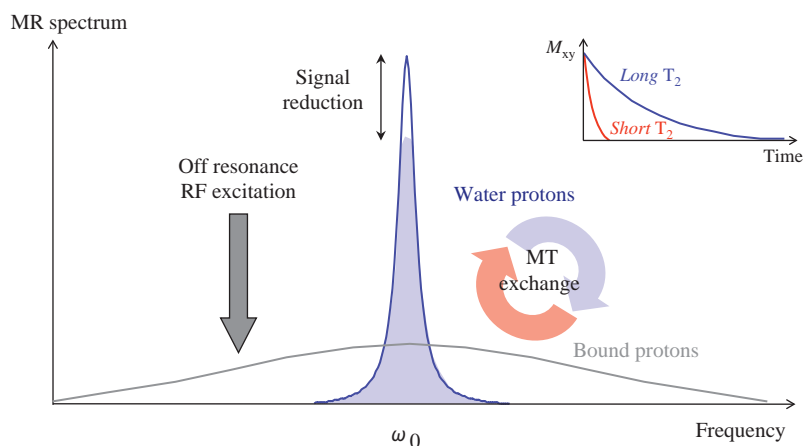
139

Figure 9.18 Magnetization transfer between bound and free protons. The free protons have long T_2 and the bound protons have a short T_2, as shown in the inset. The bound protons are not normally 'visible' in the image.

the intensity of certain tissues and improve the contrast in images. Fluids, including CSF and flowing blood, fat and bone marrow are unaffected. A major application for **MT C**ontrast (MTC) is for background suppression in time-of-flight angiography (see Chapter 15).

Getting Bound Up: MT Explained

MT contrast occurs where there is fast exchange between bound and free protons. The bound or restricted protons are those associated with macromolecules or hydration layers. This restricted pool has a very short T_2 and is invisible to direct imaging.

However, it can influence the observed MR signal through the exchange of energy (magnetization) between the two 'pools' (see Figure 9.18). The bound pool has a broad resonance and therefore can be excited by an RF pulse at a frequency several kilohertz away from the free water frequency, which therefore has no effect on the free protons. Exchange of protons between the bound and free pools means that saturated magnetization from the (invisible) bound pool will move into the free pool, thus reducing the total MR signal that can be observed.

APT and CEST

A new class of imaging techniques has been developed, based on the concept of magnetization transfer. These are known as **C**hemical **E**xchange **S**aturation **T**ransfer (CEST) imaging. CEST methods use exogenous or endogenous agents with protons which easily exchange with targeted tissues in vivo.

For example, **A**mide **P**roton **T**ransfer (APT) is a subclass of CEST that targets the proton part of the amide group (-NH-), which is available for exchange with other protons.

All these techniques use saturation at offset frequencies $\pm\Delta\omega$ on both sides of the water peak, and detect the slight drop in the water signal S_{sat} when the proton exchange occurs at one particular frequency (Figure 9.19). The saturation is achieved using a long pseudo-continuous RF train of pulses, typically lasting several seconds. The saturation train is followed by an image acquisition, for example EPI, multi-slice TSE, or 3D gradient echo. This is known as *z-spectrum imaging*, and typically generates 7–9 images at a few ppm either side of water. The saturation effect is very small, so it is common to process the images and generate an asymmetry map pixel-by-pixel:

$$MTR_{asym} = 1 - \frac{S_{sat}(\Delta\omega)}{S_{sat}(-\Delta\omega)}$$

CEST methods are very sensitive to both B_1 and B_0 inhomogeneities, and additionally take several minutes to acquire because it is necessary to sample several offset frequencies. Several CEST agents, including APT, show promise for good sensitivity in detecting malignant tumours. APT is also sensitive to changes in pH, which is potentially useful in acute stroke since lactic acid accumulates in the infarct core.

J-coupling is an interaction between the hydrogen nuclei on neighbouring atoms, which causes a splitting of the resonance peak. It is particularly important
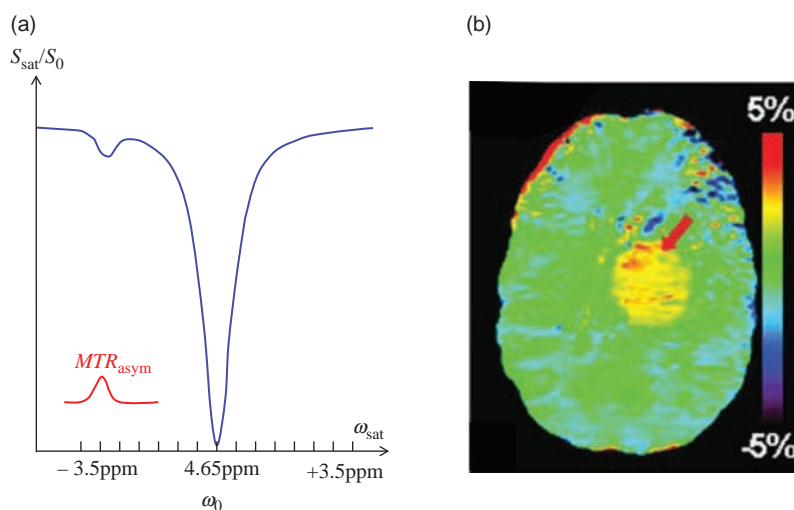
Figure 9.19 CEST imaging exploits the chemical exchange of protons between endogenous agents (in this case the amide group) and other tissues. (**a**)The amide proton resonates at 8.25 ppm, so $\Delta\omega$ is varied between ±4 ppm to capture the saturation transfer. (**b**) The MTR_{asym} image shows high signal in active tumour.

in fat molecules that contain long chains of carbon atoms. If the protons are saturated, usually by repeated RF pulses at relatively short TRs, they become decoupled and the split peak collapses to a single peak. The single peak has a higher amplitude and is narrower than the split peak, corresponding to a longer T_2. The difference between *J*-coupled and *J*-decoupled signals can be seen by comparing turbo spin echo (TSE) T_2-weighted images to conventional spin-echo (SE) T_2-weighted images. The TSE images have brighter fat signals than they should because the protons are decoupled and their T_2 is apparently lengthened. In the conventional SE images, *J*-coupling in the lipids reduces their T_2 and they have a darker appearance.

9.7 Gadolinium-based Contrast Agents

Now that you have a good idea of the relaxation mechanisms in MR, it is time to look more closely at the effect of gadolinium-containing contrast agents. In Chapter 3 we mentioned that there are other contrast agents for MRI, based on super-paramagnetic iron oxides or manganese; however, many of these have been withdrawn by manufacturers so we will not waste our time discussing the SPIOs or manganese.

By now you already know that gadolinium is a paramagnetic element. It has seven unpaired electrons in its electronic structure and becomes quite strongly magnetized when placed in a magnetic field, whereas most body tissues are diamagnetic and only become weakly magnetized. Gadolinium is toxic in its elemental state, so for MRI use it is always chelated to a ligand (a large inert molecule). You can think of these complexes as safe chemical 'wrappers' around the gadolinium atom which eliminate toxicity but preserve its paramagnetic properties.

When a gadolinium contrast agent is injected into the body, it is distributed via the vasculature to all perfused tissues. Although it is too large a molecule to cross the blood–brain barrier quickly, it does slowly leak out into the brain tissues, but rapidly accumulates in lesions where the blood–brain barrier is disrupted. In most other organs it passes from the vasculature into the interstitial space relatively quickly. After the initial redistribution into the extracellular fluid space with a half-life of about 11 min, gadolinium is gradually excreted via the kidneys with a biological half-life of approximately 90 min, so in most patients it is not detectable in tissues after about 6 h although it may linger in the urine and bladder for a day.

The effect of the strongly paramagnetic gadolinium is to decrease T_2 and T_1 relaxation times of protons in the immediate vicinity of the molecule. In this respect gadolinium behaves just like any magnetic field inhomogeneity but acting over a very small distance not much larger than the complex itself. As these protons exchange with other protons (see Section 9.6) further away from the gadolinium complex there is an overall reduction of T_1 and T_2. At low concentrations such as those used in normal clinical practice, the major effect is the T_1 shortening (see Figure 9.20), and tissues which take up the agent have enhanced signal intensity on T_1-weighted images.
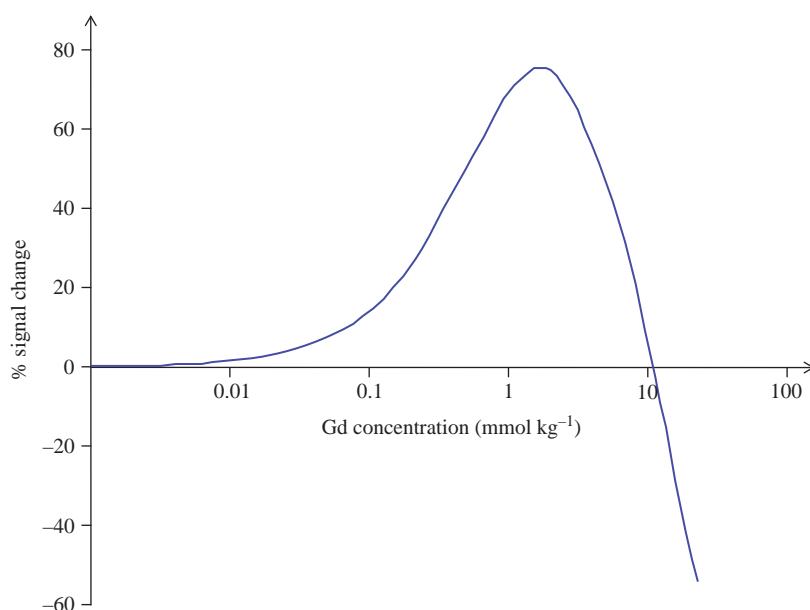
141

Figure 9.20 Signal intensity versus concentration of gadolinium, calculated using a T_1-weighted SE sequence (TR = 400 ms, TE = 15 ms) and a tissue with $T_1 = 800$ ms and $T_2 = 75$ ms.

Dosage varies depending on the particular formulation, and to some extent the body area being imaged, but in general a dose of 0.1 mmol Gd per kilogram of body weight is used. Doses for children should always be adjusted based on the child's weight. Double-dose injections may be used for MR angiography, viability and perfusion imaging and have been shown to improve the conspicuity of lesions in multiple sclerosis and metastatic disease. Recent awareness about the link between Gd and a disease called **N**ephrogenic **S**ystemic **F**ibrosis (NSF) has made the MRI community more cautious about very high doses (see Section 20.7).

There are several different formulations available commercially with various osmolalities and safety profiles (see Table 20.7). In general, gadolinium is a safe drug well tolerated by subjects, and apart from NSF there are only a handful of serious adverse effects noted in the literature. The main contraindications are poor renal function (with glomerular filtration rate <30 ml min^{-1}), and pregnancy. The gadolinium complex crosses the placenta into the fetal circulation and there is insufficient safety data about fetal exposure to gadolinium. Gadolinium also crosses into breast milk, so lactating mothers should not breast-feed for 24 h following gadolinium administration. Full details of contraindications and clinical applications can be found on the information insert in any preparation of gadolinium.

142

Contrast Agent Relaxivity

The effect of contrast agents on tissue relaxation times is best described using relaxation rates rather than times. The relaxation rate is simply the inverse of the relaxation time, so we can define

$$R_1 = \frac{1}{T_1} \qquad R_2 = \frac{1}{T_2} \qquad R_2^* = \frac{1}{T_2^*}$$

Relaxation rates are additive, so for example we can redefine the effective transverse relaxation rate as

$$R_2^* = R_2 + \frac{1}{2}\gamma\varDelta B_0$$

For contrast agents we can define a specific relaxivity r, which describes how much they change relaxation rates per molar concentration. Multiplying the specific relaxivity by the concentration in a particular tissue gives the increase in relaxation rate caused by the contrast agent, so the new relaxation rate will be

$$R' = R + rC$$

The relaxivity r may be different for longitudinal and transverse relaxation rates (usually denoted r_1 and r_2 respectively), but in the case of gadolinium they are approximately the same, 4 and 5 mmol^{-1} s^{-1} respectively. Thus at a concentration of 0.1 mmol kg^{-1} in a tissue with a T_1 of 700 ms and T_2 of 75 ms, we can calculate the new relaxation times

$$R_1' = R_1 + r_1 C = \frac{1}{0.700} + 4 \cdot 0.1 = 1.828 \Rightarrow T_1'$$

$$= \frac{1}{1.828} = 0.547 \text{ s}$$

$$R_2' = R_2 + r_2 C = \frac{1}{0.075} + 5 \cdot 0.1 = 13.833 \Rightarrow T_2'$$

$$= \frac{1}{13.833} = 0.072 \text{ s}$$

As you can see, at this concentration the biggest effect is the reduction of T_1 from 700 ms to 547 ms, whereas T_2 only changes from 75 to 72 ms. We say that the relaxation rate due to the gadolinium dominates the effective T_1 relaxation, while for transverse relaxation the normal T_2 is the dominant relaxation rate.

See also:

- Image contrast: Chapter 3
- Quality control: Chapter 11
- In vivo spectroscopy: Chapter 17

Further Reading

Abragam A (1983) *The Principles of Nuclear Magnetism*. Oxford: Clarendon Press, chapters I, II and III.

Bernstein MA, King KF and Zhou XJ (2004) *Handbook of MRI Pulse Sequences*. London: Elsevier Academic Press, chapters 4 and 6.

Brown RW, Cheng YCN, Haacke EM, Thompson MR and Venkatesan R (2014) *Magnetic Resonance Imaging: Physical Principles and Sequence Design*, 2nd edn. Hoboken, NJ: John Wiley & Sons, chapters 2–6 and 8.

Elster AD and Burdette JH (2001) *Questions and Answers in Magnetic Resonance Imaging*, 2nd edn.

London: Mosby-Yearbook, chapter 2. Also on the web at http://mri-q.com [accessed 23 March 2015].

Farrar TC and Becker ED (1971) *Pulse and Fourier Transform NMR: Introduction to Theory and Methods*. New York: Academic Press, chapters 1, 2 and 4.